# Dynamics of Survival of Motor Neuron (SMN) Protein Interaction with the mRNA-Binding Protein IMP1 Facilitates Its Trafficking into Motor Neuron Axons

**Claudia Fallini,[1,2] Jeremy P. Rouanet,[1]* Paul G. Donlin-Asp,[1]* Peng Guo,[1,3] Honglai Zhang,[3] Robert H. Singer,[3] Wilfried Rossoll,[1] Gary J. Bassell[1,4]**

[1] Department of Cell Biology, Emory University School of Medicine, Atlanta, Georgia 30322

[2] Department of Neurology, UMASS Medical School, Worcester, Massachusetts 01605

[3] Department of Anatomy and Structural Biology, Albert Einstein College of Medicine, Bronx, New York 10461

[4] Department of Neurology and Center for Neurodegenerative Diseases, Emory University School of Medicine, Atlanta, Georgia 30322

*Received 13 May 2013; revised 24 June 2013; accepted 11 July 2013*

**ABSTRACT:** **Spinal muscular atrophy (SMA) is a lethal neurodegenerative disease specifically affecting spinal motor neurons. SMA is caused by the homozygous deletion or mutation of the *survival of motor neuron 1* (*SMN1*) gene. The SMN protein plays an essential role in the assembly of spliceosomal ribonucleoproteins. However, it is still unclear how low levels of the ubiquitously expressed SMN protein lead to the selective degeneration of motor neurons. An additional role for SMN in the regulation of the axonal transport of mRNA-binding proteins (mRBPs) and their target mRNAs has been proposed. Indeed, several mRBPs have been shown to interact with SMN, and the axonal levels of few mRNAs, such as the *β-actin* mRNA, are reduced in SMA motor neurons. In this study we have identified the *β-actin* mRNA-binding protein IMP1/ZBP1 as a novel SMN-interacting protein. Using a combination of biochemical assays and quantitative imaging techniques in primary motor neurons, we show that IMP1 associates with SMN in individual granules that are actively transported in motor neuron axons. Furthermore, we demonstrate that IMP1 axonal localization depends on SMN levels, and that SMN deficiency in SMA motor neurons leads to a dramatic reduction of IMP1 protein levels. In contrast, no difference in IMP1 protein levels was detected in whole brain lysates from SMA mice, further suggesting neuron specific roles of SMN in IMP1 expression and localization. Taken together, our data support a role for SMN in the regulation of mRNA localization and axonal transport through its interaction with mRBPs such as IMP1.** © 2013 Wiley Periodicals, Inc. Develop Neurobiol 74: 319–332, 2014

***Keywords:*** **SMA; SMN; IMP1; axon; mRNA binding proteins**

Additional Supporting Information may be found in the online version of this article.

*The authors contributed equally to this work.

*Correspondence to:* G.J. Bassell (gbassel@emory.edu) or W. Rossoll (wrossol@emory.edu).

Contract grant sponsor: SMA Europe fellowship (to C.F.) and Families of SMA grant (to C.F. and W.R.).

Contract grant sponsor: National Institutes of Health (NIH); contract grant numbers: NS066030 (to W.R.), HD055835 (to G.J.B.), and training grant T32GM008367 (to P.G.D.-A.).

Contract grant sponsor: Muscular Dystrophy Association; contract grant number: 254779 (to G.J.B.).

Contract grant sponsor: Spinal Muscular Atrophy Foundation (to G.J.B.) and Weisman Family Foundation (to G.J.B. and R.H.S.).

Contract grant sponsor: Emory Neuroscience NINDS Core Facilities; contract grant number: P30NS055077.



Published online 29 July 2013 in Wiley Online Library (wileyonlinelibrary.com).
DOI 10.1002/dneu.22111

## INTRODUCTION

Spinal muscular atrophy (SMA) is a neurodegenerative disease characterized by progressive degeneration of spinal motor neurons, resulting in proximal muscle weakness and paralysis. SMA is the leading genetic cause of infant mortality, and results from the homozygous deletion or mutation of the *survival of motor neuron 1* (*SMN1*) gene (Lefebvre et al., 1995; Melki, 1999; Wirth et al., 2006). Humans carry a near-identical duplicated version of *SMN1*, *SMN2*. However, a single C to T transition in *SMN2* causes aberrant splicing and skipping of exon 7 in 80 to 90% of its transcripts, resulting in a truncated and unstable SMNΔ7 protein (Lorson et al., 1999).

The *SMN1* gene encodes for a 38 KDa protein whose best understood function is in the assembly of spliceosomal ribonucleoproteins (snRNPs). As part of a multiprotein complex comprising seven Gemin proteins (Gemin 2–8) and Unrip, SMN promotes the recognition and interaction of Sm proteins with U snRNAs, acting as a specificity factor for their efficient assembly (Pellizzoni et al., 2002). As a consequence of SMN deficiency, alteration in the splicing pattern of several pre-mRNAs has been observed in different tissues of SMA animal models (Gabanella et al., 2007; Zhang et al., 2008; Lotti et al., 2012). However, the link between these defects and the selective motor neuron loss in SMA remains unclear (Burghes and Beattie, 2009; Rossoll and Bassell, 2009; Bäumer et al., 2009). Besides its role in splicing, SMN has been proposed to regulate the interaction between mRNA-binding proteins (mRBPs) and their target mRNAs into ribonucleoprotein particles (mRNPs). We and others have demonstrated that SMN interacts with several mRBPs (reviewed in Fallini et al., 2012), including hnRNP R (Rossoll et al., 2002), KSRP (Tadesse et al., 2008), and HuD (Akten et al., 2011; Fallini et al., 2011; Hubers et al., 2011). These interactions between SMN and mRBPs can affect target mRNA stability and protein expression; however, the requirement of SMN for the localization of a specific mRBP has only been shown so far for HuD (Fallini et al., 2011). Furthermore, we have previously demonstrated that low levels of SMN severely impair the axonal localization of polyA mRNAs in motor neurons (Fallini et al., 2011), supporting a role for SMN as a general regulator of mRNP assembly and/or transport. To date, few mRNAs have been shown to be downregulated and/or mislocalized in SMN-deficient neurons. These include the *cpg15/neuritin* (Akten et al., 2011), $p21^{cip1/waf1}$ (Olaso et al., 2006; Tadesse et al., 2008; Wu et al., 2011), and *β-actin* mRNAs (Rossoll et al., 2003). In particular, the localization and translation of the *β-actin* mRNA in growth cones and axons have been shown to be necessary for axonal guidance, maintenance and regeneration (Yao et al., 2006; Vogelaar et al., 2009; Donnelly et al., 2013), suggesting that the dysregulation of *β-actin* mRNA transport and local protein synthesis may play an important role in the axonal pathogenesis of SMA.

The ability of the *β-actin* mRNA to localize to the tip of neurites requires the presence of a conserved *cis*-regulatory element in its 3' untranslated region, termed the "zipcode" (Kislauskis et al., 1994). The chicken zipcode binding protein 1 (ZBP1) and its mammalian ortholog insulin-like growth factor mRNA-binding protein 1 (IMP1), have been shown to directly control the transport and local translation of the *β-actin* mRNA in fibroblasts and neurons (Ross et al., 1997; Farina et al., 2003; Tiruchinapalli et al., 2003), regulating the axon's ability to respond to neurotrophins and guidance cues (Zhang et al., 2001; Huttelmaier et al., 2005; Welshhans and Bassell, 2011) as well as injury signals (Donnelly et al., 2011, 2013).

Interestingly, IMP1 has been shown to be part of a ribonucleoprotein complex with the neuronal mRBP HuD, regulating the axonal localization of several mRNAs, including the *β-actin*, the *microtubule associated protein tau*, and *growth-associated protein 43* (*GAP-43*) mRNAs (Atlas et al., 2004; Yoo et al., in press). These data taken together suggest a general role of SMN to facilitate the assembly and/or localization of an mRNP transport granules containing IMP1, HuD and their target mRNAs. However, it was unknown whether IMP1 interacted with SMN as well as with HuD in individual granules. In this study, we have investigated whether SMN interacts with IMP1 and is required for IMP1 localization in axons of motor neurons. IMP1, HuD, and SMN were shown to interact in individual granules that are actively transported in motor neuron axons. Furthermore, we show that SMN acute knockdown specifically affects IMP1 protein levels in the axons of motor neurons, while SMN chronic depletion in motor neurons isolated from a severe SMA mouse model leads to a downregulation of IMP1 in all cell compartments. Taken together our results support a role for SMN in regulating IMP1 mRNP localization and mRNA local translation in motor neuron axons.

## MATERIALS AND METHODS

### Primary Motor Neuron Culture and Transfection

Primary motor neurons from wild-type E13.5 mouse embryos were isolated, cultured, and transfected by magnetofection as previously described (Fallini et al., 2010). The rat IMP1 cDNA was fused C-terminally to the monomeric red fluorescent protein mCherry. A flexible linker [$(SGGG)_3$] was inserted between the fusion partners to facilitate correct protein folding. The shRNA vectors (Open Biosystems) for SMN knock down were used as described (Fallini et al., 2010). SMA motor neurons were isolated from E13.5 embryos from *Smn*$^{-/-}$*; hSMN2* transgenic mice as described (Oprea et al., 2008).

### Cell Staining and Imaging

Motor neurons were fixed for 15 min with 4% paraformaldehyde in PBS after 3, 5, or 7 days *in vitro* (DIV), as indicated. Mouse (1:500; BD) and rabbit (1:500, Santa Cruz) anti-SMN, guinea pig anti-IMP1 (1:300, Santangelo et al., 2009), mouse anti-HuD (1:500; 16C12, Santa Cruz), rabbit anti-Gemin2 (1:1000; provided by Dr. Fischer, University of Wuerzburg, Germany), and mouse anti-Unrip (1:500; BD) antibodies were incubated overnight at 4°C. Cy3-, Cy2- or Cy5-conjugated IgG species specific secondary antibodies (Jackson Immunoresearch) were incubated for 1 h at room temperature. Fluorescence *in situ* hybridization was performed as described (Fallini et al., 2011). Z-series (5 to 10 sections, 0.2 μm thickness) were acquired with an epifluorescence microscope (Ti, Nikon) equipped with a cooled CCD camera (HQ2, Photometrics). Fluorescence Z-stacks were deconvolved (Autodeblur, Media Cybernetics) and analyzed as previously described (Fallini et al., 2011). For colocalization and fluorescence intensity analysis, 70 to 80 μm of the axon starting from the cell body were analyzed. Growth cones were identified as the tip of the longest axonal branch.

### Live Cell Imaging

Motor neurons were plated on poly-ornithine/laminin coated Delta T culture dishes (Bioptechs). Twenty-four hours after transfection, cells were starved in plain Neurobasal medium for 30 min and then transport was stimulated for 15 min with either BDNF (10 ng/μL) or Br-cAMP (100 μ*M*) (Calbiochem) in glia-conditioned low fluorescence-imaging medium (Hibernate E, Brain Bits) supplemented with 2% B27 and 2% horse serum. Movies were acquired using a widefield microscope (TE2000, Nikon) with a high-speed cooled CCD camera (Cascade 512b, Photometrics) or a confocal microscope (A1R, Nikon). Particle tracking was performed using the Imaris image analysis software. Kymographs were generated using the ImageJ plugin MultipleKymograph.

### GST-Binding Assay, Co-Immunoprecipitation, and Western Blots

GST-binding assays were performed as previously described (Fallini et al., 2011). Briefly, the expression of GST-SMN and GST-IMP1 was induced in the BL21 *Escherichia coli* strain using IPTG (1 m*M*) for 3 h. Glutathione sepharose beads (GE Healthcare) bound to GST-SMN or GST-IMP1 were incubated with the protein extracts from rat brain tissues at 4°C overnight. After washing with TBS containing 500 m*M* NaCl, proteins from the bead pellets (IP) and supernatant (Spn) were run on 4 to 12% gradient gels for western blot analysis. For endogenous SMN and IMP1 protein co-immunoprecipitation, E13.5 mouse brains were lysed in lysis buffer (50 m*M* Tris-HCl, 150 m*M* NaCl, 2% Triton X-100, protease inhibitors). Immunoprecipitations with SMN (anti-SMN 2B1, Sigma) and IMP1 (MBL) antibodies was performed using protein A-agarose beads (Roche) following manufacturer's recommendations. Mouse IgGs (Sigma) were used as a control. For RNase treatment, protein extracts were incubated with or without 1 mg/mL RNase A for 1 h at 37°C before immunoprecipitation. FLAG-tagged and EGFP-tagged proteins were expressed in HEK293 cells transfected using Lipofectamine 2000 (Invitrogen) according to manufacturer's recommendations. Immunoprecipitation experiments were performed as described (Fallini et al., 2011). Monoclonal antibodies to FLAG (1:4000, Sigma) or EGFP (1:5000, BD Biosciences) were used for detection of FLAG- and EGFP-fusion proteins.

### Bimolecular Fluorescence Complementation

The PCR fragments encoding the N- and C-terminal fragments of Venus yellow fluorescent protein (VFP, a kind gift from Dr. Miyawaki, Brain Science Institute, Japan) split at nucleotide 465 (Shyu et al., 2006), were fused to full length murine SMN or SMNΔT, and full length rat IMP1 or IMP1ΔKH cDNAs. A point mutation (A206K) was introduced to generate a monomeric form of VFP as described (Zacharias et al., 2002). Neuro2a cells were transfected with TurboFect (Fermentas) as described (Fallini et al., 2011). Twelve hours after transfection, cells were fixed with 4% paraformaldehyde in PBS and 3D stacks (10–20 sections, 0.6 μm thickness) were acquired using a widefield fluorescence microscope (TE2000, Nikon). More than 100 cells per condition from three independent experiments were quantified. Fluorescence from CFP was used to identify transfected cells and to normalize the VFP signal.

### Fluorescence Recovery After Photobleaching

Fluorescence images of cells were acquired on a confocal laser scanning microscope (Nikon A1R). Venus BiFC fluorescent proteins were excited with a 488nm laser and detected using a 525/50 band pass filter. The images were taken with a Plan Apo 60× oil immersion objective with

pixel size 0.12 μm. The images were also taken with line average of 2 to minimize random noises. Photobleaching of select regions of interest (ROI) (4 μm radius circle) with a 488 nm laser at 100% power (20 s) achieved near complete loss of signal. The shape and size of the bleached spot were kept constant for all experiments. After photobleaching, fluorescence images were acquired with a 30-s interval for 30 min excited with a 488 nm laser at low (0.5%) power. Control experiments were done with low laser power so that no bleaching was observed. The recovery of fluorescence intensity was analyzed in each ROI using ImageJ to obtain intensity values at different time frames. To analyze the fluorescence recovery, the mean intensity of a defined area outside the cells was measured to define the background fluorescence and this was subtracted from each image. Percent recovery was obtained by dividing the background subtracted differences during postbleaching over prebleaching ($I_{spot} - I_{bkgd}$(postbleach)/$I_{spot} - I_{bkgd}$(prebleach)). The resulting normalized data were then averaged for 16 different ROIs in nine different cells per condition. Half-maximal time points for each treatment were calculated by using the regression equations derived from the best-fit curve of the recovery time points and calculating for 50% recovery ($y = 0.5$).

## RESULTS

### The mRNA-Binding Protein IMP1 is Localized and Actively Transported to Motor Neuron Axons

The mRNA binding protein IMP1/ZBP1 has been previously shown to localize to the axonal processes of sensory and cortical neurons (Zhang et al., 2001; Tiruchinapalli et al., 2003; Donnelly et al., 2011;

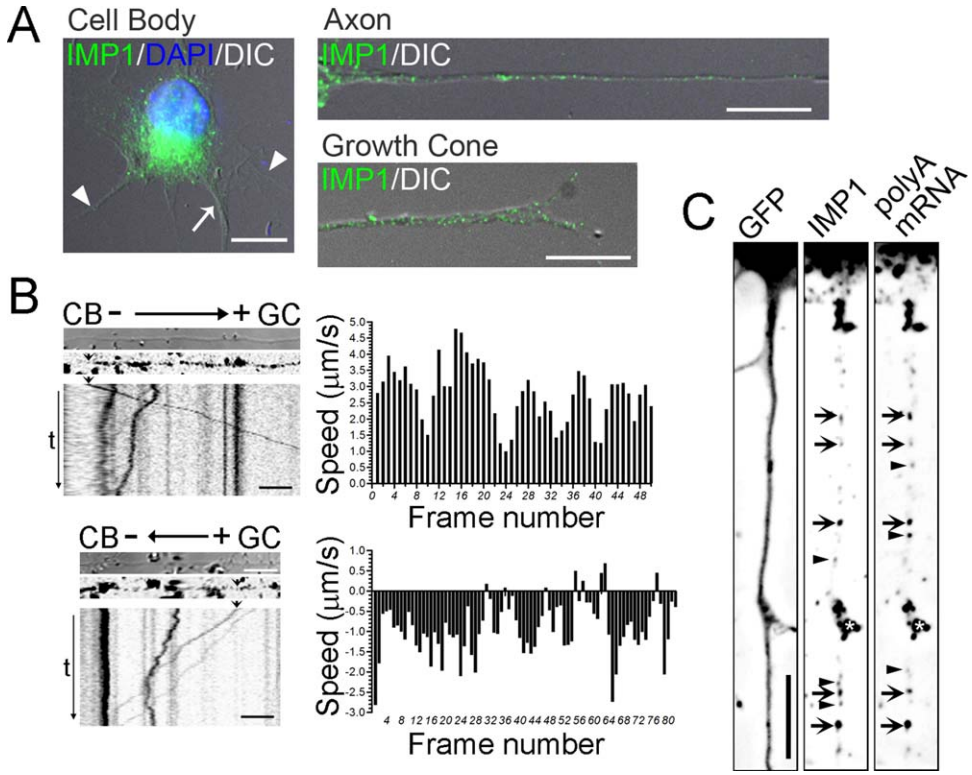


**Figure 1** IMP1 is a component of mRNPs localized and actively transported in motor neuron axons. (A) Primary motor neurons (5DIV) were stained with an antibody specific for IMP1 (green). Granular staining was observed in the cell body and dendrites (left panel), proximal axon (top right), and growth cone (bottom right). The arrow indicates the axon, while arrowheads point at dendrites. DIC images were superimposed to the fluorescence image. DAPI (blue) indicates the cell nucleus. (B) mCherry-IMP1 particles are actively transported both anterogradely (top panel; CB, cell body; GC, growth cone) and retrogradely (bottom) along motor neuron axons. Kymographs (left panels) show the particles movement over time (*t*). For each frame, the instantaneous velocity of the particles was plotted (right). (C) Endogenous IMP1 granules colocalize with poly(A) mRNAs in motor neuron axons. Arrows indicate colocalized particles, while arrowheads identify IMP1-only or poly(A) mRNA-only granules. GFP expression was used to highlight the whole cell structure. Asterisks indicate beads used for cell transfection. Scale bars: 10 μm. [Color figure can be viewed in the online issue, which is available at wileyonlinelibrary.com.]

Welshhans and Bassell, 2011). To investigate whether IMP1 was similarly distributed in motor neurons, we performed immunofluorescence experiments on primary cultured embryonic motor neurons [Fig. 1(A)]. We found that IMP1 is distributed in a granular pattern along the proximal and distal axon, as well as in dendrites. Live cell imaging analysis of motor neurons transfected with mCherry-tagged IMP1 showed that IMP1-positive fluorescent particles were actively moving both anterogradely and retrogradely along the motor axon [Fig. 1(B) and Supporting Information Fig. 1], with an average speed of $2.1 \pm 0.6$ μm/s and $1 \pm 0.1$ μm/s, respectively, in accordance with what previously observed in cortical neurons (Welshhans and Bassell, 2011). Furthermore, fluorescence *in situ* hybridization using oligodT probes specific to the total poly(A) mRNA population revealed a strong colocalization between IMP1 and poly(A) mRNAs [Fig. 1(C)]. Together, these data demonstrate that IMP1 is part of RNA granules that are actively transported in motor neuron axons.

## IMP1 Specifically Interacts with SMN *In Vitro* and *In Vivo*

In order to investigate whether IMP1 associated with SMN-positive granules in motor neuron axons, we performed GST-pull down and co-immunoprecipitation

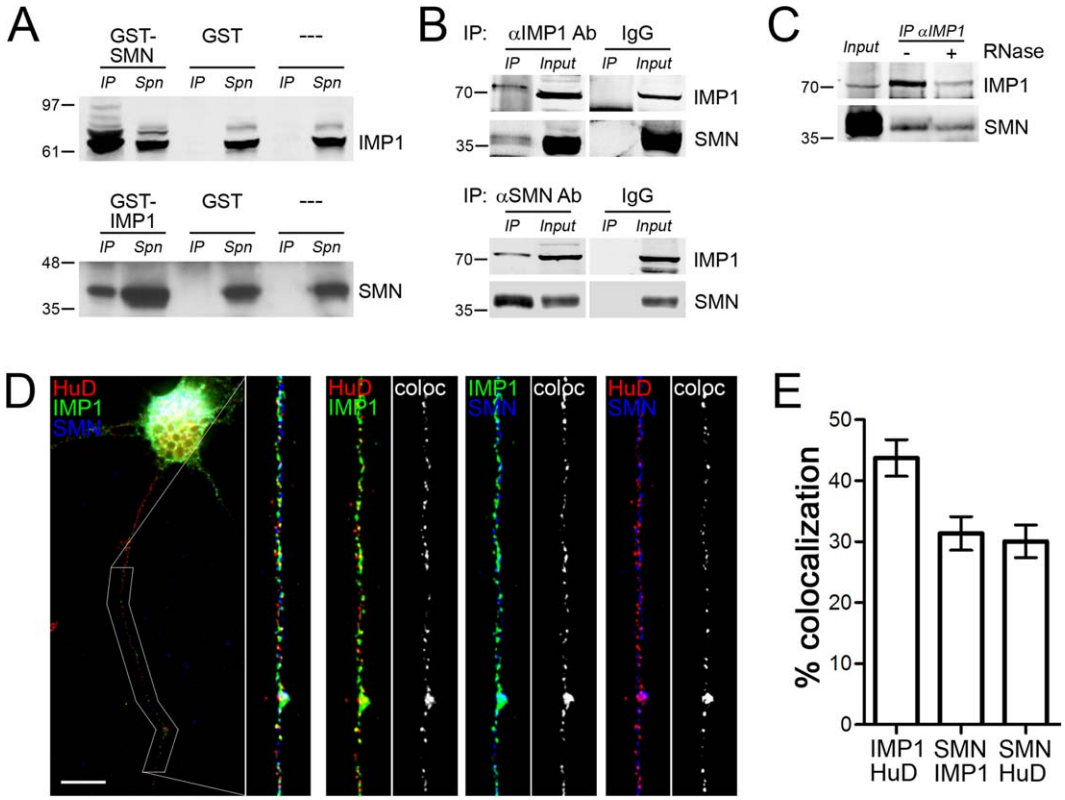


**Figure 2** IMP1 associates with HuD and SMN and co-localizes in axonal granules. (A) GST-immunoprecipitation (IP) assays show that GST-tagged SMN (top panel) and GST-tagged IMP1 (bottom) co-purify with endogenous IMP1 and SMN from whole brain protein lysates. GST and beads only (-) were used as controls for the IP specificity. Spn, supernatant; IP, immunoprecipitate. (B) Endogenous IMP1 (top panel) and SMN (bottom) were specifically immunoprecipitated from embryonic mouse brain lysates. Co-purification of SMN (top, *IP*) and IMP1 (bottom, *IP*) respectively was observed. The input represents the protein lysate used for the IP. IgGs were used as control. (C) RNase treatment (1 mg/mL) does not affect IMP1 co-immunoprecipitation of SMN from brain lysate. (D) Triple label immunofluorescence detection of IMP1 (green), SMN (blue), and HuD (red) for quantitative colocalization analysis in primary motor neurons (5DIV). A representative image is shown. The axon was straightened and enlarged to show colocalization between IMP1-HuD (left panel), IMP1-SMN (middle), and HuD-SMN (right). Colocalized pixels are shown in white (coloc). Scale bar: 10 μm. (E) Percentage of protein colocalization was quantified from 30 cells from three independent experiments. Bars represent mean and SEM. [Color figure can be viewed in the online issue, which is available at wileyonlinelibrary.com.]

(co-IP) experiments [Fig. 2(A–C)]. First, brain extracts were incubated with GST-tagged IMP1 or SMN recombinant proteins. Endogenous SMN and IMP1 were co-purified with GST-IMP1 and GST-SMN respectively, but not with the GST or beads-only controls [Fig. 2(A)]. Second, endogenous SMN and IMP1 proteins were immunoprecipitated from brain lysates, and the co-purified proteins were tested for the presence of IMP1 and SMN. Strong bands corresponding to IMP1 and SMN were visible in the SMN and IMP1 IPs respectively, but not in the IgG control lanes [Fig. 2(B)]. Furthermore, we could demonstrate that SMN-IMP1 interaction is not RNA-dependent, as no effect on the co-IP was observed following RNase treatment of the brain protein extract [Fig. 2(C)]. To further confirm and extend these results in cultured neurons, a stringent colocalization analysis was performed. Primary motor neurons were labeled by immunofluorescence with antibodies specific for endogenous IMP1 and SMN. Additionally, the colocalization of IMP1 with HuD was investigated, as HuD has been previously shown to interact with IMP1 (Atlas et al., 2004; Yoo et al., in press) and SMN (Akten et al., 2011; Fallini et al., 2011; Hubers et al., 2011). Interestingly, we found that 31.4% of SMN granules were also positive for IMP1, similarly to what we observed for SMN and HuD (30.1%) [Fig. 2(D,E)], and 43.7% IMP1 granules also contained HuD, supporting what previously observed in other cell types (Atlas et al., 2004; Yoo et al., in press). Additionally we found that about 50% of SMN-IMP1 granules also contained HuD (not shown). Collectively, our data suggest that IMP1, SMN, and HuD are common components of macromolecular complexes that are present in motor neuron axons.

## IMP1 Associates with the SMN Complex in Mobile Axonal Granules

Since we showed that IMP1 is actively transported in motor neuron axons where it colocalizes with SMN, we next investigated whether SMN and IMP1 are indeed part of the same particle rather than being in two distinct but associated granules. To this end, we employed the bimolecular fluorescence complementation (BiFC) technique (Ventura, 2011) that, as we have previously shown, allows to discriminate between associated proteins that are closely interacting versus distant components of the same complex (Fallini et al., 2011). In this technique, the N- and C-terminal non-fluorescent halves of the yellow fluorescent protein Venus (VFP) are fused to two potentially interacting proteins. If these proteins are in very close proximity (i.e., in the same complex), the VFP halves will complement and fluoresce. When primary motor neurons were transfected with the BiFC constructs for HuD and IMP1, a specific granular signal was observed in the cell body and along the axonal process, confirming the colocalization analysis. Similarly, when the BiFC constructs for SMN and IMP1 were co-expressed in motor neurons, fluorescent puncta were visible in the cell body and axon but not in the nucleus [Fig. 3(A)]. Furthermore, live cell imaging revealed that SMN-IMP1 BiFC granules are actively transported along the neuron axon [Fig. 3(B), Supporting Information Fig. 2] with an average speed of $1.6 \pm 0.8$ μm/s and $1.4 \pm 0.4$ μm/s in the anterograde and retrograde directions respectively, thus suggesting that IMP1 and SMN are part of the same motile RNA transport granules.

Since we have previously shown that SMN, Gemin2, Unrip, and HuD are part of a multiprotein complex that is actively transported in motor axons (Fallini et al., 2011), we examined whether IMP1 may be an additional component of the same complex. Toward this end, motor neurons transfected with the SMN-IMP1 BiFC pair were immunostained with antibodies specific for the endogenous HuD, Gemin2, and Unrip proteins. A strong colocalization was observed in all three cases [Fig. 3(C)]. To test whether the interaction of IMP1 with the SMN complex depended on the presence of SMN, HEK293 cells were transfected with FLAG-IMP1, EGFP-tagged Gemin2 and Gemin3, and with or without EGFP-SMN. When all four proteins were co-expressed, the three members of the SMN complex were co-purified with IMP1 [Fig. 3(D)]. However, if EGFP-SMN was not present, no co-IP of Gemin2 and Gemin3 with IMP1 was observed, suggesting that SMN is necessary for the association of IMP1 with the SMN multiprotein complex.

## SMN Tudor Domain and IMP1 KH-Domains are Necessary for SMN-IMP1 Interaction

To investigate what protein domains are involved in the interaction between SMN and IMP1, we generated SMN deletion constructs lacking SMN exon 7 (SMNΔ7), the Tudor domain (SMNΔT), the N-terminus (SMNΔN53), or both the exon 7 and the N-terminus (SMNΔN53Δ7). Co-immunoprecipitation experiments showed that the SMN Tudor domain is necessary and sufficient for the SMN-IMP1 interaction [Fig. 4(A,B)]. Indeed, the deletion of the Tudor domain abolished SMN-IMP1 co-purification, while no effect was evident when the other protein domains were absent. Additionally, we showed that FLAG-tagged IMP1 could

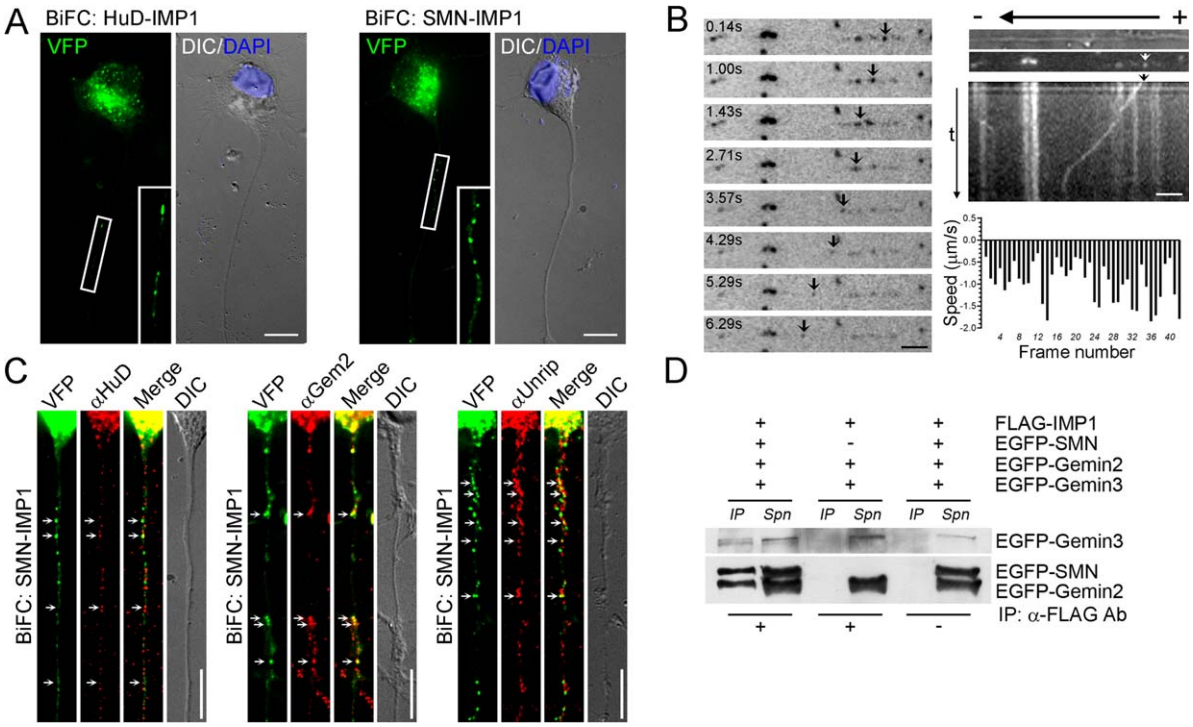


**Figure 3** BiFC reveals IMP1 association with SMN and HuD within individual particles in axons of motor neurons. (A) Primary motor neurons (2DIV) were transfected with BiFC constructs for IMP1-HuD (left panel) or IMP1-SMN (right panel). In both conditions, BiFC signal (green) was detected in the cell body and axon, while no BiFC granules were present in the nucleus (blue, DAPI). (B) Live cell imaging of motor neurons transfected with the BiFC pair SMN-IMP1 revealed active transport of BiFC-positive granules along motor neuron axons. Movie snapshots (left panel) and kymograph (right) of a representative particle are shown. For each frame, the instantaneous velocity of the particle was plotted. (C) Axonal SMN-IMP1 BiFC granules colocalize with endogenous HuD (arrows, left panel), Gemin2 (arrows, middle panel), and Unrip (arrows, right panel) detected by imunofluorescence. Scale bars: 10 μm. (D) IMP1 associates with the SMN-Gemin multiprotein complex via SMN. FLAG-IMP1 was co-transfected with EGFP-tagged Gemin2, Gemin3, and with or without EGFP-SMN in HEK293 cells. IMP1 IP with the FLAG antibody co-purified EGFP-Gemin2 and EGFP-Gemin3 in the presence of EGFP-SMN (lanes 1–2). However if EGFP-SMN was not co-expressed, no co-IP of Gemin2 and Gemin3 was observed (lanes 3–4). As control, beads only were used for the IP (lanes 5–6). [Color figure can be viewed in the online issue, which is available at wileyonlinelibrary.com.]

selectively co-precipitate the SMN Tudor domain alone [Fig. 4(B)]. To further confirm these results, we employed quantitative BiFC. Neuro2a cells were transfected with full length SMN-IMP1 BiFC pairs, and the VFP fluorescence intensity was measured in individual transfected cells [Fig. 4(C)]. The fluorescence intensity of the co-transfected cyan fluorescent protein (CFP) was used to normalize the data. Using this assay, we tested the effects of the deletion of the SMN Tudor domain and of the four IMP1 KH domains (IMP1ΔKH), since these RNA-binding domains are essential for IMP1 interaction with *β-actin* mRNA (Farina et al., 2003). Interestingly, we found that the deletion of the SMN Tudor domain and of the IMP1 KH domains significantly reduced SMN-IMP1 interaction, with a dramatic shift of the VFP/CFP ratio in the cell population towards lower values. To investigate whether the deletion of the Tudor domain also negatively impacted the dynamics of the SMN-IMP1 interaction, we performed fluorescence recovery after photobleaching (FRAP) experiments [Fig. 4(D)]. Neuro2a cells were transfected with the BiFC constructs for IMP1 and full length SMN or SMNΔT. Twenty-four hours after transfection, BiFC-positive cells were photobleached at select regions of interest containing fluorescent puncta using a 488 nm laser at 100% power, and the reoccurrence of the VFP fluorescence was monitored every 30 s over a period of 30 min. We found that when the SMN Tudor domain was deleted, the normalized fluorescence recovery time was three times longer compared with the full-length protein.

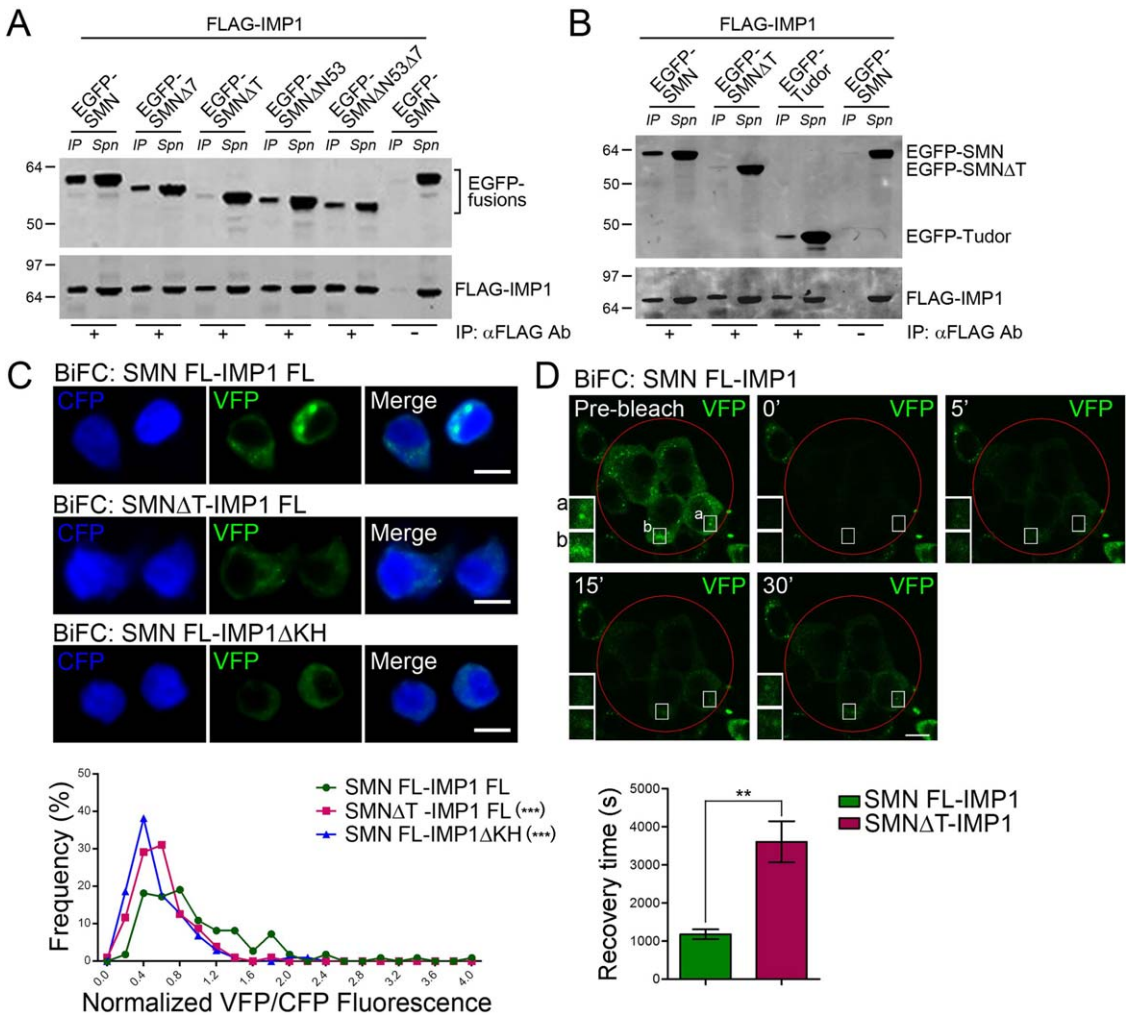


**Figure 4** The SMN Tudor domain and IMP1 KH domains are necessary for SMN-IMP1 interaction. (A and B) FLAG-IMP1 and various EGFP-SMN deletion constructs were co-expressed in HEK293 cells. IMP1 was specifically precipitated using an anti-FLAG antibody. IMP1 and SMN co-IP was impaired by the deletion of SMN Tudor domain (SMNΔT), while the deletion of SMN exon 7 (SMNΔ7), N-terminus (SMNΔN53), or both (SMNΔN53Δ7) had no effect (A). The SMN Tudor domain alone fused to EGFP was also selectively purified with FLAG-IMP1 (B). Monoclonal GFP and FLAG antibodies were used for detection. A beads-only negative control (−) was used for the IP. (C) BiFC was used to detect SMN-IMP1 interaction in cells. Neuro2a cells were transfected with BiFC constructs for full length SMN (SMN FL) or SMNΔT and full-length IMP1 (IMP1 FL) or IMP1ΔKH. Representative cells are shown. The BiFC signal (VFP, green) is significantly reduced in cells expressing IMP1 or SMN deletion constructs compared with the full length protein. CFP (blue) was used to identify transfected cells and normalize VFP fluorescence intensity. The VFP and CFP fluorescence intensity was measured in more than 100 cells from three independent experiments. The frequency distribution of the VFP/CFP ratio was plotted for the three conditions. A significant shift of the distribution toward lower values was observed when the SMNΔT or the IMP1ΔKH were expressed (Kolmogorov-Smirnov test, $n = 105$, $^{***}p < 0.001$). (D) FRAP experiments further show that the deletion of SMN Tudor domain affects the dynamics of SMN-IMP1 association. Representative images show transfected Neuro2a cells before (pre-bleach) and after photobleaching (0, 5, 15, and 30 min) of the BiFC signal (VFP, green). The red circle indicates the bleached region. The fluorescence recovery time was measured in cells transfected with IMP1 and with either full length SMN or SMNΔT. Bars represent mean and SEM (Student's $t$-test, $n = 9$, $^{**}p < 0.01$). [Color figure can be viewed in the online issue, which is available at wileyonlinelibrary.com.]

Taken together, these results indicate that both the SMN Tudor domain and IMP1 KH domains are necessary for mediating SMN-IMP1 protein binding and for regulating the dynamics of their interaction at specific loci within the cytoplasm.

## SMN Knock Down Affects IMP1 Axonal Localization

We and others have shown that low levels of SMN lead to defects in the localization and/or reduction in overall levels of its interacting proteins (Jablonka et al., 2001; Wang and Dreyfuss, 2001; Helmken et al., 2003; Tadesse et al., 2008; Fallini et al., 2011). To test whether also IMP1 protein levels are dependent on SMN levels, we acutely knocked down the SMN protein in wild type motor neurons by using a vector-based shRNA strategy (Fig. 5) (Fallini et al., 2010, 2011). Motor neurons were transfected with an shRNA construct targeting SMN (shSMN) or a non-silencing control (shCtrl), and fixed 5 days after transfection. SMN and IMP1 protein levels were then evaluated by quantitative immunofluorescence. Compared with the control cells, primary motor neurons transfected with the shSMN vector showed a dramatic reduction in SMN levels both in the cell body ($1 \pm 0.07$ shCtrl *vs.* $0.64 \pm 0.06$ shSMN; $n = 30$; Student's *t*-test, $p < 0.001$) and in the proximal axon ($1 \pm 0.16$ shCtrl *vs.* $0.63 \pm 0.07$ shSMN; $n = 30$; Student's *t*-test,

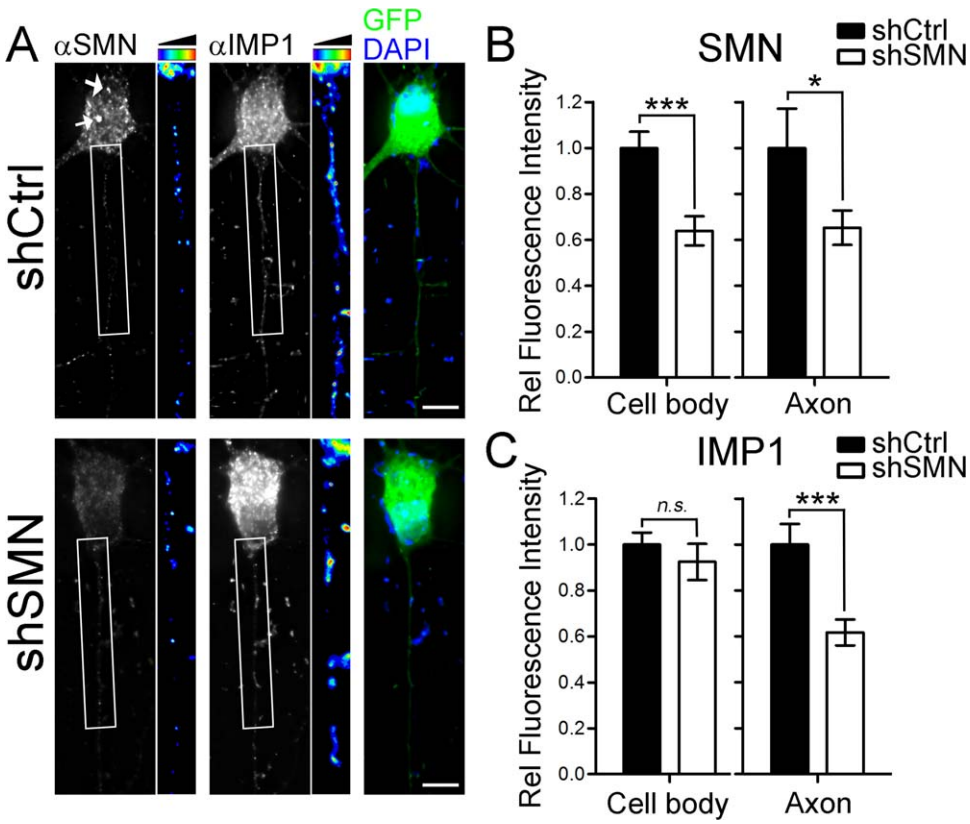


**Figure 5** Axonal IMP1 protein levels are reduced upon SMN knockdown. (A) Representative images showing primary motor neurons transfected with either shCtrl (top panel) or shSMN (bottom panel) constructs and labeled by immunofluorescence for endogenous SMN (left panel) and IMP1 (center panel) 5 days after transfection. GFP (green, right panel) was used to identify transfected cells. Nuclei were labeled with DAPI (blue). Arrows indicate SMN-positive nuclear gems. Axons were straightened and pseudo-colored with a 16-bit intensity map. Scale bars: 10 μm. (B and C) Quantification of SMN levels showed a significant 36% and 37% reduction of SMN protein levels in the cell bodies and axons of shSMN treated motor neurons relative to control (B). Conversely, IMP1 protein levels were significantly reduced in the axon (61% *vs.* shCtrl), but not the cell body (92% *vs.* shCtrl), of shSMN treated motor neurons (C). Bars represent mean and SEM (Student's *t*-test, $*p < 0.05$, $***p < 0.001$). [Color figure can be viewed in the online issue, which is available at wileyonlinelibrary.com.]

$p < 0.05$). Interestingly, we found that SMN knockdown did not affect IMP1 levels in the cell body ($1 \pm 0.05$ shCtrl *vs.* $0.92 \pm 0.07$ shSMN; $n = 40$; Student's *t*-test, $p = 0.4$), while a 39% reduction in IMP1 levels in the axon was observed ($1 \pm 0.08$ shCtrl *vs.* $0.61 \pm 0.05$ shSMN; $n = 43$; Student's *t*-test, $p < 0.001$). These results strongly suggest that SMN, by interacting with IMP1, favors its axonal localization, without effect on total levels of IMP1 upon acute knockdown.

## SMN Deficiency Affects IMP1 Protein Levels in Motor Neurons

In order to investigate the effects of SMN loss in a model that more closely mimics SMA, we performed immunofluorescence analysis of IMP1 distribution in motor neurons isolated from a severe SMA mouse model (*Smn*$^{-/-}$*;hSMN2*) (Monani et al., 2000). Motor neurons isolated from wild type (WT) or SMA embryos were fixed five days after plating, and SMN and IMP1 levels in the cell body, proximal, and distal

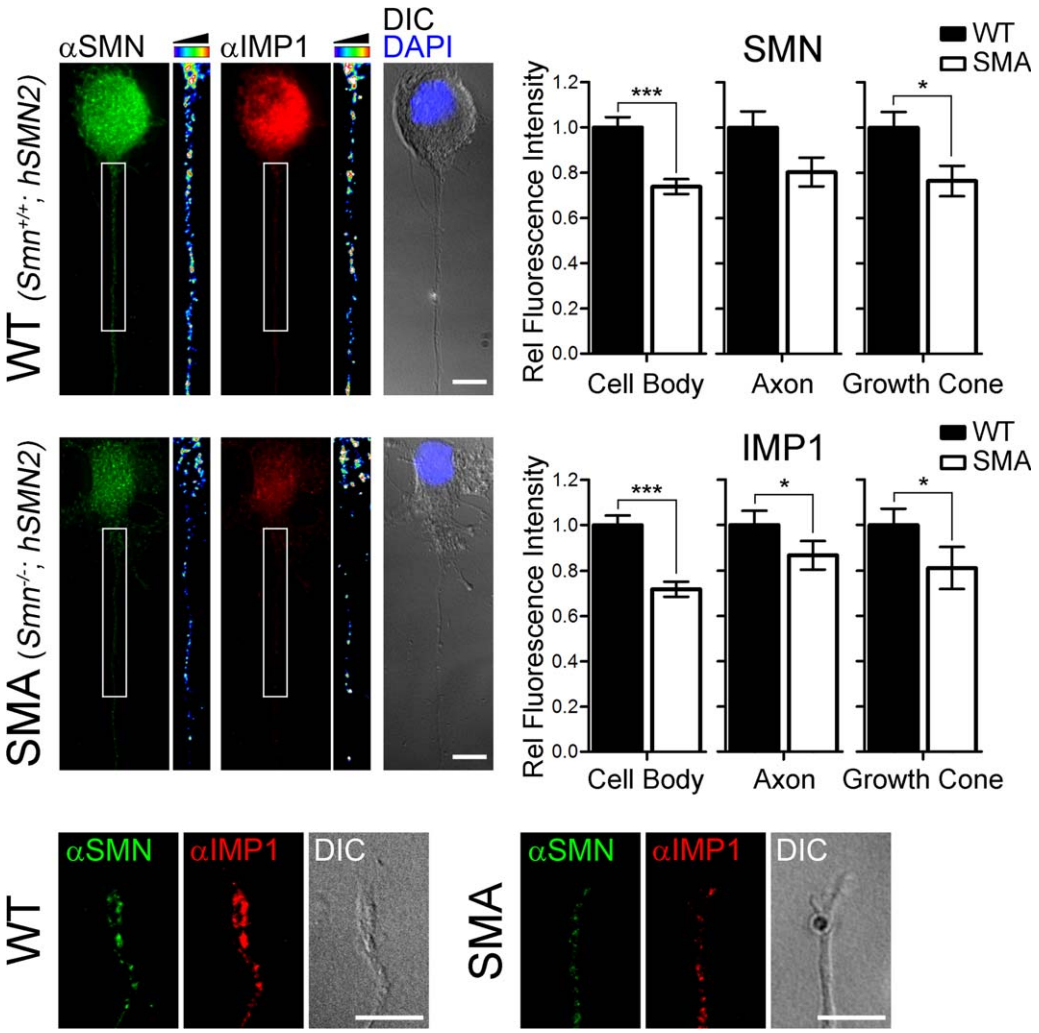


**Figure 6** IMP1 protein levels are reduced in SMA motor neurons. (A) Primary motor neurons (5DIV) derived from WT (*Smn*$^{+/+}$*; hSMN2*) and SMA (*Smn*$^{-/-}$*; hSMN2*) littermates were immunostained for endogenous IMP1 (red) and SMN (green). Representative images are shown for the cell body and proximal axon (top two panels) and growth cone segments (bottom panels). Axons were straightened and pseudo-colored with a 16-bit intensity map. Quantification of SMN levels showed a significant reduction of SMN protein levels in both the cell bodies and growth cones of SMA motor neurons relative to WT cells. Similarly, the quantification of IMP1 levels showed a significant reduction in the cell bodies, axons, and growth cones of SMA motor neurons relative to WT controls. Bars represent mean and SEM (Student's *t*-test, $*p < 0.05$, $***p < 0.001$). Scale bars: 10 μm. [Color figure can be viewed in the online issue, which is available at wileyonlinelibrary.com.]

axon were evaluated by quantitative immunofluorescence (Fig. 6). As expected, SMN levels were significantly reduced in the cell body and growth cone (cell body: $1 \pm 0.04$ WT *vs.* $0.72 \pm 0.03$ SMA, $n = 55$, Student's *t*-test, $p < 0.001$; growth cone: $1 \pm 0.07$ WT *vs.* $0.81 \pm 0.09$ SMA, $n = 48$, Student's *t*-test, $p < 0.05$), while the reduction in SMN levels in the proximal axon did not reach statistical significance due to a high variability ($1 \pm 0.06$ WT *vs.* $0.87 \pm 0.06$ SMA, $n = 53$, Student's *t*-test, $p = 0.08$). Surprisingly, when IMP1 levels were quantified, a significant reduction was observed in all cell compartments (cell body: $1 \pm 0.04$ WT *vs.* $0.74 \pm 0.03$ SMA, $n = 55$, Student's *t*-test, $p < 0.001$; axon: $1 \pm 0.07$ WT *vs.* $0.8 \pm 0.06$ SMA, $n = 53$, Student's *t*-test, $p < 0.05$; growth cone: $1 \pm 0.06$ WT *vs.* $0.76 \pm 0.07$ SMA, $n = 48$, Student's *t*-test, $p < 0.05$), suggesting that SMN deficiency over time in an end-stage disease model may lead to IMP1 instability and degradation.

## IMP1 Protein Levels are not Altered in SMA Brain Lysates

Since both SMN and IMP1 are ubiquitously expressed, we sought to investigate whether reduced levels of IMP1 due to SMN depletion are a general effect in neuronal tissues. To test this possibility, we quantified IMP1 protein levels in brain protein extracts isolated from WT and SMA mice at E13.5 (Fig. 7). As expected, SMA brain lysates were significantly depleted of the full length SMN protein ($0.18 \pm 0.06$ SMA *vs.* WT; $n = 4$; paired *t*-test, $p < 0.05$). However, we did not observe any significant difference in the overall IMP1 levels ($0.87 \pm 0.26$ SMA *vs.* WT; $n = 4$; paired *t*-test, $p = 0.33$). This result suggests that the reduced IMP1 levels observed in SMN-deficient motor neurons are a specific defect that is not common to all cell types.

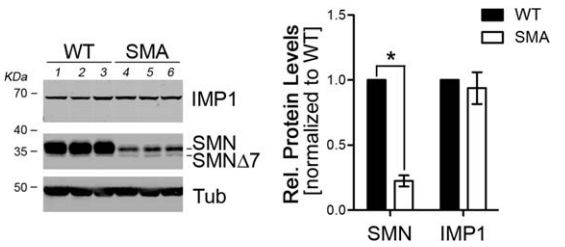


**Figure 7** Endogenous IMP1 protein levels are unchanged in the brain of SMA mice. Western blot analysis of IMP1 (top), SMN (middle) and tubulin (Tub, bottom) levels from E13.5 WT or SMA brain lysate reveals IMP1 protein levels to be unchanged. As expected, SMN levels are greatly diminished in SMA embryos. The SMNΔ7 protein product from the SMN2 transgene is also visible. SMN and IMP1 band intensities were normalized to tubulin from five independent experiments. Bars represent mean and SEM (Student's *t*-test, $*p < 0.05$).

## DISCUSSION

In this study we have characterized the interaction of the spinal muscular atrophy (SMA) disease protein SMN with the mRNA-binding protein (mRBP) IMP1, and the role of SMN in promoting IMP1 localization to motor neuron axons. SMN protein is part of a macromolecular complex—the SMN complex—that plays an essential housekeeping role in the assembly of spliceosomal small nuclear ribonucleoproteins (snRNPs) by favoring the high-fidelity binding of Sm proteins to U snRNAs. Despite many efforts to connect this essential function to SMA pathogenesis, the evidence for its role in the disease mechanism is still inconclusive (Burghes and Beattie, 2009; Rossoll and Bassell, 2009). In parallel to an essential and ubiquitous function of SMN in splicing, we and others have proposed a noncanonical role for the SMN complex in the assembly of mRBPs and their target mRNAs into messenger ribonucleoprotein complexes (mRNPs) (Briese et al., 2005; Rossoll and Bassell, 2009; Fallini et al., 2012). In support to this hypothesis, several mRBPs with well-established roles in mRNA regulation have been shown to interact with SMN and other members of the SMN complex (reviewed in Fallini et al., 2012). Using a combination of biochemical assays and quantitative imaging techniques in primary motor neurons, here we have demonstrated that IMP1 interacts with SMN in axonal granules that are actively transported along the neuronal processes. We have shown that this interaction depends on the presence of the SMN Tudor domain, a known protein-protein interaction domain which is responsible for SMN association with other mRBPs, such as HuD (Akten et al., 2011; Fallini et al., 2011; Hubers et al., 2011) and KSRP (Tadesse et al., 2008), as well as SMN interaction with Sm proteins (Selenko et al., 2001). Additionally, we could show that IMP1-SMN axonal granules contain other members of the SMN complex, such as Gemin2 and Unrip, thus providing support for the proposed dual role of SMN in snRNP and mRNP assembly. We have previously shown that SMN interacts with the mRBP HuD in the axon of motor neurons (Fallini et al., 2011). Interestingly, IMP1 and HuD have been shown to colocalize with the *β-actin* and *GAP-43* mRNAs (Yoo et al., in press), and to cooperate in the regulation of the axonal transport and local translation of *tau* mRNA (Atlas et al.,

2004). Our results clearly demonstrate that both IMP1 and HuD are present in the axonal SMN-positive granules, thus identifying these particles as mRNPs and providing further evidence for SMN noncanonical function in motor neuron axons.

A functional significance for SMN interaction with mRBPs comes from the observation that the acute depletion of SMN in wild-type motor neurons leads to the impairment of IMP1 axonal localization. A similar phenotype caused by SMN depletion has been previously observed for HuD (Fallini et al., 2011), suggesting that SMN may act as a facilitator of mRBPs localization and possibly active transport in the axon of motor neurons. Interestingly, when we investigated the effects of chronically low levels of SMN in an SMA mouse model on the localization of IMP1, a reduction of the protein levels in all cell compartments, including the distal growth cone, was detected. This observation suggests that over time the functional impairment of IMP1 and other mRBPs due to their axonal mislocalization caused by SMN loss may lead to a reduction of their protein levels, thus severely affecting the regulation of mRNA transport and/or local translation. Furthermore, the negative effect of SMN depletion on IMP1 levels was not observed in whole brain tissues, suggesting that this effect is not a general phenomenon occurring in all cell types, but it may be specific to neurons. It will be interesting to see whether IMP1 axonal mislocalization in SMA is a phenotype common to all neuronal types or rather unique to motor neurons.

Since motor neurons have very long axons with elaborate synaptic terminals, the cellular machinery regulating RNA transport and local translation is expected to be particularly important for the function and maintenance of these cells (Wiersma-Meems et al., 2005; Lasiecka et al., 2009; Wang et al., 2010; Swanger and Bassell, 2011), as it is also underscored by the involvement of mRBPs in another motor neuron disease, amyotrophic lateral sclerosis (Polymenidou et al., 2012). We and others have shown that SMN deficiency leads to a severe impairment in the localization and/or stability of few specific mRNAs, including the *β-actin* mRNA (Rossoll et al., 2003). Our observation that IMP1, the major protein regulating *β-actin* mRNA localization and translation (Ross et al., 1997; Farina et al., 2003; Tiruchinapalli et al., 2003), is first mislocalized and later downregulated in motor neurons due to low levels of SMN may thus provide a mechanistic explanation for the observed defects in *β-actin* mRNA localization. Indeed, limited availability of the IMP1 protein in DRG neurons has been shown to severely affect the axonal levels the *β-actin* mRNA (Donnelly et al., 2011), and cortical neurons isolated from IMP1 knockout mice display severe defects in the levels of locally synthesized β-actin protein at the growth cones (Welshhans and Bassell, 2011). Together, these data support a pathogenic role for IMP1 axonal mislocalization in SMA. However, the defective localization of *β-actin* mRNA alone is not likely to be responsible for the neurodegeneration that characterizes SMA. As suggested by the dramatic reduction in the poly(A) mRNA levels in SMN-depleted motor neuron axons (Fallini et al., 2011), the deregulation of a wide array of mRNAs at both the pre- and postsynaptic compartment of motor neurons is expected to contribute to SMA. Several SMN-interacting mRBPs and mRNAs are predicted to be mislocalized and downregulated as a result of SMN depletion. Likely candidates are the *microtubule-associated protein tau* and the *growth-associated protein 43* (*GAP43*). Together with *β-actin*, these mRNAs are bound and regulated by HuD and IMP1, whose synergistic activity controls their stability and axonal transport.

In conclusions, our results support the hypothesis that SMN plays a noncanonical role in the regulation of mRNP assembly and in their axonal localization in cultured motor neurons. Further characterization of SMN interaction with other mRBPs and the identification of their target mRNAs that are mislocalized or downregulated in SMA motor neurons, both *in vitro* and *in vivo*, will be needed to understand the full extent and mechanisms of the axonal dysregulation of mRNA, leading to selective motor neuron degeneration in SMA.

The authors thank Dr. Yukio Sasaki and Dr. Utz Fischer for providing antibodies. The authors also thank Lian Li and Latoya Rowe for excellent technical support.

## REFERENCES

Akten B, Kye MJ, Hao le T, Wertz MH, Singh S, Nie D, Huang J, et al. 2011. Interaction of survival of motor neuron (SMN) and HuD proteins with mRNA cpg15 rescues motor neuron axonal deficits. Proc Natl Acad Sci U S A 108:10337–10342.

Atlas R, Behar L, Elliott E, Ginzburg I. 2004. The insulin-like growth factor mRNA binding-protein IMP-1 and the Ras-regulatory protein G3BP associate with tau mRNA and HuD protein in differentiated P19 neuronal cells. J Neurochem 89:613–626.

Bäumer D, Lee S, Nicholson G, Davies JL, Parkinson NJ, Murray LM, Gillingwater TH, et al. 2009. Alternative splicing events are a late feature of pathology in a mouse model of spinal muscular atrophy. PLoS One 5:e1000773.

Briese M, Esmaeili B, Sattelle DB. 2005. Is spinal muscular atrophy the result of defects in motor neuron processes? Bioessays 27:946–957.

Burghes AH, Beattie CE. 2009. Spinal muscular atrophy: Why do low levels of survival motor neuron protein make motor neurons sick? Nat Rev Neurosci 10:597–609.

Donnelly CJ, Park M, Spillane M, Yoo S, Pacheco A, Gomes C, Vuppalanchi D, et al. 2013. Axonally synthesized beta-actin and GAP-43 proteins support distinct modes of axonal growth. J Neurosci 33:3311–3322.

Donnelly CJ, Willis DE, Xu M, Tep C, Jiang C, Yoo S, Schanen NC, et al. 2011. Limited availability of ZBP1 restricts axonal mRNA localization and nerve regeneration capacity. EMBO J 30:4665–4677.

Fallini C, Bassell GJ, Rossoll W. 2010. High-efficiency transfection of cultured primary motor neurons to study protein localization, trafficking, and function. Mol Neurodegener 5:17.

Fallini C, Bassell GJ, Rossoll W. 2012. Spinal muscular atrophy: The role of SMN in axonal mRNA regulation. Brain Res 1462:81–92.

Fallini C, Zhang H, Su Y, Silani V, Singer RH, Rossoll W, Bassell GJ. 2011. The survival of motor neuron (SMN) protein interacts with the mRNA-binding protein HuD and regulates localization of poly(A) mRNA in primary motor neuron axons. J Neurosci 31:3914–3925.

Farina KL, Huttelmaier S, Musunuru K, Darnell R, Singer RH. 2003. Two ZBP1 KH domains facilitate beta-actin mRNA localization, granule formation, and cytoskeletal attachment. J Cell Biol 160:77–87.

Gabanella F, Butchbach ME, Saieva L, Carissimi C, Burghes AH, Pellizzoni L. 2007. Ribonucleoprotein assembly defects correlate with spinal muscular atrophy severity and preferentially affect a subset of spliceosomal snRNPs. PLoS One 2:e921.

Helmken C, Hofmann Y, Schoenen F, Oprea G, Raschke H, Rudnik-Schoneborn S, Zerres K, et al. 2003. Evidence for a modifying pathway in SMA discordant families: Reduced SMN level decreases the amount of its interacting partners and Htra2-beta1. Hum Genet 114:11–21.

Hubers L, Valderrama-Carvajal H, Laframboise J, Timbers J, Sanchez G, Cote J. 2011. HuD interacts with survival motor neuron protein and can rescue spinal muscular atrophy-like neuronal defects. Hum Mol Genet 20:553–579.

Huttelmaier S, Zenklusen D, Lederer M, Dictenberg J, Lorenz M, Meng X, Bassell GJ, et al. 2005. Spatial regulation of beta-actin translation by Src-dependent phosphorylation of ZBP1. Nature 438:512–515.

Jablonka S, Bandilla M, Wiese S, Buhler D, Wirth B, Sendtner M, Fischer U. 2001. Co-regulation of survival of motor neuron (SMN) protein and its interactor SIP1 during development and in spinal muscular atrophy. Hum Mol Genet 10:497–505.

Kislauskis EH, Zhu X, Singer RH. 1994. Sequences responsible for intracellular localization of beta-actin messenger RNA also affect cell phenotype. J Cell Biol 127:441–451.

Lasiecka ZM, Yap CC, Vakulenko M, Winckler B. 2009. Compartmentalizing the neuronal plasma membrane from axon initial segments to synapses. Int Rev Cell Mol Biol 272:303–389.

Lefebvre S, Burglen L, Reboullet S, Clermont O, Burlet P, Viollet L, Benichou B, et al. 1995. Identification and characterization of a spinal muscular atrophy-determining gene. Cell 80:155–165.

Lorson CL, Hahnen E, Androphy EJ, Wirth B. 1999. A single nucleotide in the SMN gene regulates splicing and is responsible for spinal muscular atrophy. Proc Natl Acad Sci USA 96:6307–6311.

Lotti F, Imlach WL, Saieva L, Beck ES, Hao le T, Li DK, Jiao W, et al. 2012. An SMN-dependent U12 splicing event essential for motor circuit function. Cell 151:440–454.

Melki J. 1999. Molecular basis of spinal muscular atrophy: recent advances. J Child Neurol 14:43.

Monani UR, Sendtner M, Coovert DD, Parsons DW, Andreassi C, Le TT, Jablonka S, et al. 2000. The human centromeric survival motor neuron gene (SMN2) rescues embryonic lethality in Smn(−/−) mice and results in a mouse with spinal muscular atrophy. Hum Mol Genet 9: 333–339.

Olaso R, Joshi V, Fernandez J, Roblot N, Courageot S, Bonnefont JP, Melki J. 2006. Activation of RNA metabolism-related genes in mouse but not human tissues deficient in SMN. Physiol Genomics 24:97–104.

Oprea GE, Krober S, McWhorter ML, Rossoll W, Muller S, Krawczak M, Bassell GJ, et al. 2008. Plastin 3 is a protective modifier of autosomal recessive spinal muscular atrophy. Science 320:524–527.

Pellizzoni L, Yong J, Dreyfuss G. 2002. Essential role for the SMN complex in the specificity of snRNP assembly. Science 298:1775–1779.

Polymenidou M, Lagier-Tourenne C, Hutt KR, Bennett CF, Cleveland DW, Yeo GW. 2012. Misregulated RNA processing in amyotrophic lateral sclerosis. Brain Res 1462: 3–15.

Ross AF, Oleynikov Y, Kislauskis EH, Taneja KL, Singer RH. 1997. Characterization of a beta-actin mRNA zipcode-binding protein. Mol Cell Biol 17:2158–2165.

Rossoll W, Bassell GJ. 2009. Spinal muscular atrophy and a model for survival of motor neuron protein function in axonal ribonucleoprotein complexes. Results Probl Cell Differ 48:289–326.

Rossoll W, Jablonka S, Andreassi C, Kroning AK, Karle K, Monani UR, Sendtner M. 2003. Smn, the spinal muscular atrophy-determining gene product, modulates axon growth and localization of beta-actin mRNA in growth cones of motoneurons. J Cell Biol 163:801–812.

Rossoll W, Kroning AK, Ohndorf UM, Steegborn C, Jablonka S, Sendtner M. 2002. Specific interaction of Smn, the spinal muscular atrophy determining gene product, with hnRNP-R and gry-rbp/hnRNP-Q: a role for Smn in RNA processing in motor axons? Hum Mol Genet 11:93–105.

Santangelo PJ, Lifland AW, Curt P, Sasaki Y, Bassell GJ, Lindquist ME, Crowe JE Jr. 2009. Single molecule-sensitive probes for imaging RNA in live cells. Nat Methods 6:347–349.

Selenko P, Sprangers R, Stier G, Buhler D, Fischer U, Sattler M. 2001. SMN tudor domain structure and its interaction with the Sm proteins. Nat Struct Biol 8:27–31.

Shyu YJ, Liu H, Deng X, Hu CD. 2006. Identification of new fluorescent protein fragments for bimolecular fluorescence complementation analysis under physiological conditions. Biotechniques 40:61–66.

Swanger SA, Bassell GJ. 2011. Making and breaking synapses through local mRNA regulation. Curr Opin Genet Dev 21:414–421.

Tadesse H, Deschenes-Furry J, Boisvenue S, Cote J. 2008. KH-type splicing regulatory protein interacts with survival motor neuron protein and is misregulated in spinal muscular atrophy. Hum Mol Genet 17:506–524.

Tiruchinapalli DM, Oleynikov Y, Kelic S, Shenoy SM, Hartley A, Stanton PK, Singer RH, et al. 2003. Activity-dependent trafficking and dynamic localization of zipcode binding protein 1 and beta-actin mRNA in dendrites and spines of hippocampal neurons. J Neurosci 23:3251–3261.

Ventura S. 2011. Bimolecular fluorescence complementation: illuminating cellular protein interactions. Curr Mol Med 11:582–598.

Vogelaar CF, Gervasi NM, Gumy LF, Story DJ, Raha-Chowdhury R, Leung KM, Holt CE, et al. 2009. Axonal mRNAs: Characterisation and role in the growth and regeneration of dorsal root ganglion axons and growth cones. Mol Cell Neurosci 42:102–115.

Wang DO, Martin KC, Zukin RS. 2010. Spatially restricting gene expression by local translation at synapses. Trends Neurosci 33:173–182.

Wang J, Dreyfuss G. 2001. A cell system with targeted disruption of the SMN gene: Functional conservation of the SMN protein and dependence of Gemin2 on SMN. J Biol Chem 276:9599–9605.

Welshhans K, Bassell GJ. 2011. Netrin-1-induced local beta-actin synthesis and growth cone guidance requires zipcode binding protein 1. J Neurosci 31:9800–9813.

Wiersma-Meems R, Van Minnen J, Syed NI. 2005. Synapse formation and plasticity: The roles of local protein synthesis. Neuroscientist 11:228–237.

Wirth B, Brichta L, Hahnen E. 2006. Spinal muscular atrophy: From gene to therapy. Semin Pediatr Neurol 13:121–131.

Wu CY, Whye D, Glazewski L, Choe L, Kerr D, Lee KH, Mason RW, et al. 2011. Proteomic assessment of a cell model of spinal muscular atrophy. BMC Neurosci 12:25.

Yao J, Sasaki Y, Wen Z, Bassell GJ, Zheng JQ. 2006. An essential role for beta-actin mRNA localization and translation in Ca2+-dependent growth cone guidance. Nat Neurosci 9:1265–1273.

Yoo S, Kim HH, Kim P, Donnelly CJ, Kalinski AL, Vuppalanchi D, Park M, et al. A HuD-ZBP1 ribonucleoprotein complex localizes GAP-43 mRNA into axons through its 3' untranslated region AU-rich regulatory element. J Neurochem, in press.

Zacharias DA, Violin JD, Newton AC, Tsien RY. 2002. Partitioning of lipid-modified monomeric GFPs into membrane microdomains of live cells. Science 296:913–916.

Zhang HL, Eom T, Oleynikov Y, Shenoy SM, Liebelt DA, Dictenberg JB, Singer RH, et al. 2001. Neurotrophin-induced transport of a beta-actin mRNP complex increases beta-actin levels and stimulates growth cone motility. Neuron 31:261–275.

Zhang Z, Lotti F, Dittmar K, Younis I, Wan L, Kasim M, Dreyfuss G. 2008. SMN deficiency causes tissue-specific perturbations in the repertoire of snRNAs and widespread defects in splicing. Cell 133:585–600.